ORAL DISEASES

Oral Diseases (2015) 21, 608–618 doi:10.1111/odi.12323

www.wiley.com

ORIGINAL ARTICLE

The CRISPR/Cas system inhibited the pro-oncogenic effects of alternatively spliced fibronectin extra domain A via editing the genome in salivary adenoid cystic carcinoma cells

H-C Wang[1,a], Y Yang[1,a], S-Y Xu[2], J Peng[1], J-H Jiang[3], C-Y Li[1]

[1]*The Central Laboratory, Peking University School and Hospital of Stomatology, Haidian District, Beijing;* [2]*Department of Oral Implanting, Shandong University School of Stomatology, Lixia District, Jinan;* [3]*The Department of Orthodontics, Peking University School and Hospital of Stomatology, Haidian District, China*

OBJECTIVES: To identify the association of fibronectin (FN) extra domain A (EDA) with the progression of salivary adenoid cystic carcinoma (SACC). Accordingly, the exclusion of EDA exon through the CRISPR/Cas9 system was investigated as the rescue for such pro-oncogenic splicing.

MATERIALS AND METHODS: SACC-83 cells were transiently transfected with plasmids containing recombinant EDA, and the cellular growth and motility were then accessed *in vitro*. Epithelial–mesenchymal transition (EMT) was investigated with immunohistochemistry, Western blot, and real-time PCR analysis. SACC tissues from 81 patients were used to access the associations between EDA+FN and clinical–pathological parameters. CRISPR/Cas9 plasmids containing sgRNA were designed and co-transfected into SACC-83 cells; the effects of EDA knockout on cellular growth and motility were then accessed.

RESULTS: The recombinant EDA exhibited little effect on the proliferation of SACC cells, but significantly promoted the migration and invasion of the cells ($P < 0.05$), accompanied with upregulated EMT ($P < 0.05$); consistently, the expression of EDA+FN was positively associated with the metastasis, nerve invasion and recurrence of SACC ($P < 0.05$). Furthermore, the EDA knockout from the FN gene in most SACC cells resulted in a decrease in cell motility and invasion, as well as prolonged population doubling time, compared with untreated SACC-83 cells ($P < 0.05$).

CONCLUSION: The EDA domain significantly promoted the motility of SACC cells, and positively associated with the tumor progression in patients with SACC. Thus, it is a potential risk factor and also a therapeutic target for SACC. The CRISPR/Cas9 system may control a pro-oncogenic splicing process through the exclusion of EDA exon from the FN gene, leading to inhibition of motility, invasion and proliferation of cancer cells.

Oral Diseases (2015) **21**, 608–618

Keywords: salivary adenoid cystic carcinoma; extra domain A; cellular motility; CRISPR/Cas; pro-oncogenic splicing; knockout

Introduction

The human genome contains annotations for at least 28 526 genes, in which 65% produce multiple transcripts (Pal *et al*, 2012) such as alternative variants of the oncogenes and tumor suppressor genes, which are generated by alternative splicing and intron retention (Davuluri *et al*, 2008; Rajan *et al*, 2009). The aberrant expression of one isoform over another in some of these genes is directly linked to tumor initiation and progression (Pal *et al*, 2012).

Fibronectin (FN), an important component of extracellular matrix (ECM), is also involved in alternative splicing (Manabe *et al*, 1997). The alternative splicing exon—extra domain A (EDA) – is always included as the EDA-positive fibronectin (EDA+FN) isoform in cancer, embryo and wound-healing tissues, whereas EDA is excluded in normal adult tissues (van der Straaten *et al*, 2004; McFadden *et al*, 2010). Previous studies demonstrated that the peptide motif (CTYSSPEDGIHEC) within EDA is necessary

Correspondence: Cui-Ying Li. MD, PhD, The Central Laboratory, Peking University School and Hospital of Stomatology, 22 South Zhongguancun Avenue Haidian District, Beijing 100081, China. Tel: (8610) – 13801382933, Fax: (8610) 82195769, E-mail: licuiying_67@163.com
and
Jiu-Hui Jiang, PhD, The Department of Othodontics, Peking University School and Hospital of Stomatology, 22 South Zhongguancun Avenue Haidian District, Beijing 100081, China. Tel: (8610) – 13911863598, Fax: (8610) 82195336, E-mail: drjiangw@gmail.com
[a]The authors contributed equally to this article.
Received 9 December 2014; revised 24 January 2015; accepted 2 February 2015

for the binding of integrin $\alpha 9\beta 1$ (Shinde *et al*, 2008; Sun *et al*, 2014), which in turn alters cytoskeleton and facilitates cellular adhesion, proliferation and epithelial–mesenchymal transition (EMT) in cancer cells (Liao *et al*, 2002; Ou *et al*, 2011; Sun *et al*, 2014). As one of the most common malignancies in salivary glands (Moskaluk, 2013), salivary adenoid cystic carcinoma (SACC) is characterized in aggressiveness, high rates of recurrence, and distant metastasis (Epivatianos *et al*, 2005). EDA+FN in SACC cells is increased by transforming growth factor (TGF-β) (Zhang and Li, 2007), which promotes the motility and metastasis of the SACC (Dong *et al*, 2011, 2013). Therefore, EDA may partly be involved in SACC progression, and further, perhaps a potential target for clinical treatment of cancer.

Several approaches have been applied to inhibit the pro-oncogenic alternative variants, one of which is the knockdown of abnormal variants with siRNA, such as the knockdown of KLF6-SV1 in prostate cancer (Narla *et al*, 2005). Utilization of the upstream signals to control alternative splicing is another approach, which includes upregulation of TNFα or TGF-β1 and can promote the expression of pro-angiogenic or anti-angiogenic VEGF isoforms, respectively (Nowak *et al*, 2008). Anti-sense oligonucleotides (ASOs) is used for the inhibition of abnormal splicing reaction in pre-mRNA (Bauman *et al*, 2010). However, the side effects or cytotoxicity, efficiency, and technological complexity have limited applications of these technologies (Pal *et al*, 2012; Bonomi *et al*, 2013). For instance, the knockdown of EDA+FN by siRNA actually decreases the total amount of FN (Gomes-da-Silva *et al*, 2014) although it is vital to normal tissues (Manabe *et al*, 1997).

Recently, a newly invented technology, called the CRISPR/Cas system, provided an opportunity of inhibiting the alternative variants (Jinek *et al*, 2012). In the CRISPR/Cas system, the single-guided RNA (sgRNA) complements to special DNA sites (with PAM motif) and recruits nuclease Cas for generation of double strain breaks (DSBs) (Hsu *et al*, 2013; Wang *et al*, 2013), and then directly edits or eliminates gene sequences. This system has been used *in vivo* to rescue tyrosinemia by restoring DNA mutation with acceptable efficiency and side effects (Yin *et al*, 2014). This study demonstrated the contribution of EDA to the aggressiveness and metastasis of SACC, and the elimination of EDA by the CRISPR/Cas system demonstrated its value in inhibiting pro-oncogenic alternative splicing by directly editing gene sequences.

Materials and methods

Human primary SACC samples

The formalin-fixed paraffin-embedded specimens used for immunohistochemistry were collected from 81 patients with SACC, who were diagnosed and surgically treated at the Department of Oral and Maxillofacial Surgery, Peking University School of Stomatology, from 2000 to 2013. Clinical information was taken from operative and pathological reports, and the follow-up data were obtained from the clinical database. None of patients received preoperative chemotherapy or radiotherapy. Clinical and pathological features of patients were collected by the retrospective review of medical archives. All patients provided written informed consent to use their tumor samples for research purposes as approved by the Review Board of Peking University.

Cell culture

The adenoid cystic carcinoma cell line, SACC-83, was derived from a patient pathologically diagnosed with ACC in the sublingual gland; it was established and maintained by Peking University School of Stomatology (Li, 1990). It was grown in RPMI 1640 medium (Gibco, Grand Island, NY, USA) containing 10% fetal bovine serum (FBS; Gibco) at 37°C, 5% CO_2. The EDA-encoding exon (GenBank EF550130.1) of FN gene was amplified from the cDNA samples of SACC-83 cells.

Construction and transfection with EDA containing or knockout vectors

According to a previous study (Shinde *et al*, 2008), the sequence of EDA exon was cloned into eukaryotic expression plasmid pIRES2-EGFP, inserted between the signal peptide Igk (GenBank JX002666.1) and Flag tag, making the recombinant peptide secretive and easily detectable. EDA-positive and EDA-negative (control) plasmids were confirmed by DNA sequencing. When SACC-83 cells grew to 40–60% confluence, the EDA-positive and EDA-negative plasmids were, respectively, transfected with Lipofectamine 2000 (Life Technologies, Grand Island, NY, USA) in RPMI 1640 without FBS for 6 h, and then replaced with the complete medium without penicillin and streptomycin. After 48 h of transfection, the efficiency of transfection was accessed according to the expression of green fluorescent protein (GFP), and the recombinant EDA peptide was probed with anti-Flag.

Following previous studies (Wang *et al*, 2013; Yin *et al*, 2014), two sgRNAs were designed to complement the upstream (sgRNA upstream) or downstream (sgRNA downstream) of the EDA exon at the sites with PAM sequence. As shown in Figure 4, the oligo DNA sequences encoding sgRNA were respectively annealed and cloned into PX330, a CRISPR/Cas9 plasmid preserved in Peking University from (Wang *et al*, 2013); these two sgRNA-guided CRISPR/Cas9 plasmids were confirmed by DNA sequencing. SACC-83 cells were co-transfected by the two sgRNA-guided CRISPR/Cas9 plasmids with the Lipofectamine 2000 as mentioned above. After 24 h, Puromycin (1.2 μg ml^{-1}) was added to the medium for a 48-h treatment, and 7–8 days later, genomic DNA was extracted and the efficiency of EDA knockout was accessed with PCR analysis; the EDA-negative FN gene was confirmed by DNA sequencing according to previous studies (Cong *et al*, 2013). The SACC-83 cells without any treatment were used as control. The sequences of CRISPR sgRNAs and primers used are given in Table 1.

Colony-forming unit (CFU) and population doubling time (PDT) assay

Salivary adenoid cystic carcinoma cells transfected with EDA-positive plasmids and control cells were seeded onto 100-mm dishes at the density of 1000/dish and cultured with RPMI 1640 for 7 days. Cells were then stained with crystal violet, and the aggregation of more than 50 cells counted was defined as a colony-forming unit (CFU). In addition, cells were seeded onto 96-well plates at the density of 3000 per well, and the cell number was counted daily in six wells with Cell Counting Kit-8 (Dojindo, Kumamoto, Japan) according to the manufacturer's instruction (Wang and Li, 2013).

Similarly, the EDA-knockout cells and control cells were seeded onto 100-mm dishes at the density of 400 per dish for the CFU assay and seeded onto 96-well plates at the density of 1000 per well for measuring PDT.

Cell cycle analysis

The cell cycle was analyzed by flow cytometry according to standard procedures. In brief, cells were harvested, washed, and gently resuspended in 250 μl hypotonic fluorochrome solution (PBS containing 50 μg propidium iodide, 0.1% sodium citrate, and 0.1% Triton X-100) with RNase A (100 U ml^{-1}) to stain cell nuclei. DNA content was analyzed with FACS Calibur Flow Cytometer (Becton Dickinson, Franklin Lakes, NJ, USA).

Assay for wound-healing migration and trans-well invasion

Cells were seeded in 24-well plates and grown to confluence, synchronized in RPMI 1640 medium containing 0.5% FBS, for 6 h, and wounded by a 300- to 400-μm pipette. The wounds were photographed

Table 1 Sequences of CRISPR sgRNA and confirming primers used in this study

Name	*sgRNA sequence (5′–3′)*	*PAM sequences (5′–3′)*	*DSB site in fibronectin (FN) genome (ref|NC_018913.2|)*
sgRNA upstream-F	GTTACAGACATTGATCGCCCTAA	AGG	216251686
sgRNA upstream-R	AACTTAGGGCGATCAATGTCTGT		
sgRNA downstream-F	GTTCTGATTGGAACCCAGTCCAC	AGG	216251434
sgRNA downstream-R	AACGTGGA CTGGGTTCCAATCAG		

	Primers	*Product containing EDA*	*Product without EDA*
Primer-down	atagtgggttaattggact	675 bp	400 bp
Primer-up	agggtaatcacagggag		

Table 2 The primers used for real-time PCR

Name	*Primers*	*Sequence (5′–3′)*	*Gene ID*
E-cadherin	Forward	AACGAGGCTAACGTCGTAATCA	NM_004360.3
	Reverse	CCCAGGGGACAAGGGTATGAA	
N-cadherin	Forward	CAGATAGCCCGGTTTCATTTGA	NM_001792.3
	Reverse	CAGGCTTTGATCCCTCAGGAA	
FSP1	Forward	GATGAGCAACTTGGACAGCAA	NM_002961.2
	Reverse	CTGGGCTGCTTATCTGGGAAG	
α-SMA	Forward	CGGTGCTGTCTCTCTATGCC	NM_001141945.1
	Reverse	CACGCTCAGTCAGGATCTTCA	
Snail1	Forward	GCCTTCAACTGCAAATACTGC	NM_005985.3
	Reverse	CTTCTTGACATCTGAGTGGGTC	

at 100× magnification (TE-2000 U, Nikon, Japan), and the average linear speed of movement of the wound edges was quantified over 24 h. The cell invasion assay was performed using trans-well chambers with a polycarbonate membrane (Millipore, Bedford, MA, USA), coated with 20 μg ECM gel (Sigma-Aldrich). SACC cells transfected with EDA-positive plasmids and control cells were seeded at 1×10^5 cells per well in the upper chambers; EDA-knockout cells and control cells were seeded at 4×10^4 cells per well. After 20 h of incubation, the membranes were stained with 1% crystal violet and cells on the upper surface of the membrane were wiped off.

RNA extraction, reverse transcription, and PCR amplification

Total RNA was isolated from all cells with TRIZOL Reagent (Life Technologies). 2 μg total RNA sample was reverse-transcribed into cDNA using the superscript first-strand synthesis system (Life Technologies) according to manufacturer's instructions. Reactions were conducted in a 20 μl reaction mixture with ABI 7500 real-time PCR system (ABI), including initial incubation at 95°C for 10 min, followed by 40 cycles of annealing/extension at 60°C for 1 min and denaturation at 95°C for 15 s (Wang *et al*, 2014). The expression of E-cadherin, N-cadherin, FSP1, α-SMA, and Snail1 was normalized by human β-actin expression as described previously (Wang and Li, 2013). The primers used for gene expression are described in Table 2.

Western blot analysis

Protein was extracted from cells grown in complete medium (Dong *et al*, 2011, 2013), and the supernatants collected from cell cultures deprived of serum for 24 h (Sun *et al*, 2008). Proteins were subjected to separation on 12% SDS–PAGE. The membranes were probed with the following antibodies at 4°C overnight, respectively: anti-Flag, IST-9, anti-F-actin, anti-E-cadherin, and anti-β-actin (Abcam Ltd., Cambridge, MA, USA). Immunocomplexes were detected with an enhanced chemiluminescence blotting kit (Applygen Technology Inc., Beijing, China).

Immunostaining and immunofluorescence

Cells were fixed with 95% ethanol, blocked in 1% BSA in PBS, permeabilized in 0.5% Triton X-100 in PBS, stained with 1/500 anti-F-actin monoclonal antibody (Abcam Ltd.) at 4°C overnight, and then reacted with biotinylated secondary antibody (1:200) for 1 h. The immunocomplexes were visualized with diaminobenzidine (Zhongshan Golden Bridge Biological Technology Co., Ltd, Beijing, China). The expression of F-actin was also detected by indirect immunofluorescence, and fluorescence images were obtained with DAPI excitation settings on the laser confocal microscope (Lsm 5 Exciter; Zeiss, Jena, Germany).

Immunohistochemical staining and evaluation

The primary tumor tissues of patients were sectioned into 4-μm-thick slices and stained with 1/200 mouse monoclonal [IST-9] anti-EDA+FN (Abcam Ltd.) or IgG control at 4°C overnight and subsequently reacted with biotinylated secondary antibody (1:200) for 1 h. The immunocomplexes were visualized with diaminobenzidine (Zhongshan Golden Bridge Biological Technology CO., LTD, Beijing, China). Immunoreactions were separately evaluated for the positive DAB staining by two independent pathologists (Vargas *et al*, 2008). Five views were examined per slide, and 100 cells were observed per view at X400 magnification. Cytoplasmic and nuclear immunostaining in tumor cells was considered as positive staining. The positively stained cells exhibiting EDA+FN were scored as '0' (0%), '1' (1–5%), '2' (5–25%), '3' (25–50%), and '4' (50–100%). Intensity was scored as 0 for negative, 1 for weak, 2 for moderate, and 3 for strong. The staining intensity scores plus the proportion score of positive staining cells were used to define the EDA+FN expression levels: 0–2 for low expression and 3–7 for high expression, on which patients with SACC were classified into two groups (El-Nagdy *et al*, 2013; Dai *et al*, 2014). Immunohistochemical staining was semiquantitatively analyzed by histological score (H-score) based on the positive cell number and intensity. The H-score was calculated by the following formula: 'HS = Σ Pi (1+i)/100', where the 'Pi' is the percentage of stained cells in each intensity score (0–3) (Budwit-Novotny *et al*, 1986).

Statistical analysis

Immunohistochemical data were analyzed with Spearman's correlation. The overall survival rates and disease-free survival rates in patients with SACC were estimated by Kaplan–Meier survival curves. The comparison of experimental data was made for a difference between EDA-overexpressing cells, EDA-knockout cells, and control cells. Each experiment was performed in triplicate. Quantitative data were expressed as means ± s.d. and analyzed by Student's t-test for the differences between paired groups. Statistical significance was set at $P < 0.05$ level.

Results

The overexpression of recombinant EDA fragment

The EDA-positive plasmids and EDA-negative plasmids were transfected into SACC-83 cells, respectively. After 48 h of transfection, more than 50% cells expressed green fluorescence in both groups (Figures 1a1–b2). Western blot analysis indicated that SACC cells transfected with EDA-positive plasmids overexpressed recombinant EDA that contains Flag tag, and the recombinant EDA extracted from cell lysate (about 15 kD) that contains signal peptide Igk was broken down and secreted into the supernatants (about 13 kD), while the cells transfected with EDA-negative plasmids (controls) lacked the recombinant EDA (Figure 2h).

Little effects of the recombinant EDA on proliferation of SACC cells

Both the EDA-overexpressing cells and controls were clonogenic although their proliferation might be impaired by transfection. The number of CFUs was similar between these two groups (52.4 ± 5.68/1000 cells *vs* 52.8 ± 9.96/1000 cells, $P = 0.940$) (Figures 1c1–c2 and 2a). Similarly, the PDT between the above two groups was also approximate (52.59 ± 5.08 h *vs* 49.97 ± 5.62 h, $P = 0.417$) (Figure 2b, c), suggesting little effect of recombinant EDA on the SACC cell proliferation. Furthermore, there was no significant difference in the proportion of cells at the G0/G1, S, and G2/M phases between EDA-overexpressing and control cells (Figures 2d1–d2) (Table 3), suggesting the lack of effects on the cell cycle.

Recombinant EDA promoted the motility of SACC cells via initiating epithelia–-mesenchymal transition (EMT)

The wound-healing assay indicated that EDA-overexpressing cells had an increase in motility with speed of 7.23 ± 2.53 $\mu m\ h^{-1}$ compared with controls (3.73 ± 0.54 $\mu m\ h^{-1}$, $P = 0.0167$) (Figures 1d1–e2 and 2e). Consistently, the former exhibited significantly higher invasive ability than the latter (166.75 ± 17.29 per field *vs* 96.88 ± 13.29 per field; $P < 0.01$) (Figures 1f1–f2 and 2f). Simultaneously, EDA-overexpressing cells exhibited more membrane ruffles, lamellipodia, and filopodia extensions than controls, in which the F-actin filaments mainly concentrated around the nucleus (Figure 1i1–i2), as described previously (Ou *et al*, 2011; Guillot and Lecuit, 2013).

As the cell motility was increased by overexpression of recombinant EDA, there were a series of genes reflecting epithelial–mesenchymal transition (EMT), as illustrated in Table 4. Correspondingly, both the mRNA and protein levels of E-cadherin were significantly decreased in EDA-overexpressing cells (Figure 2g, h), suggesting the

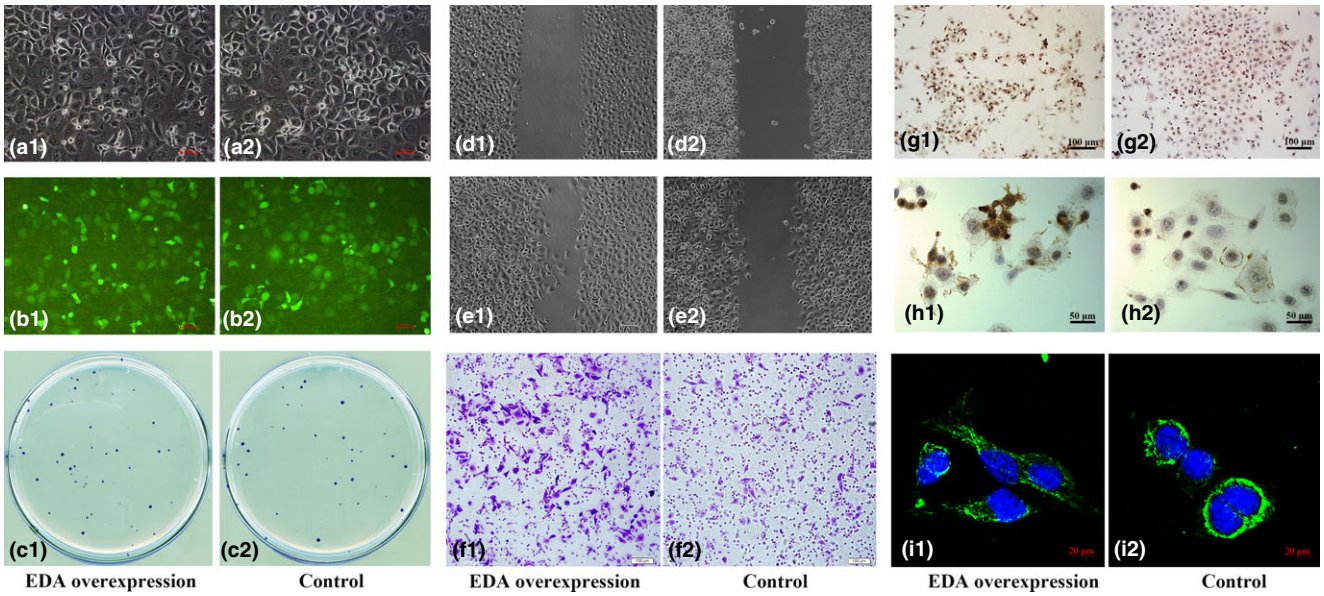

Figure 1 The transfection efficiency of the plasmids containing recombinant EDA (**a1**, **b1**), as well as the control plasmid (**a2**, **b2**) (with original magnification ×100, scale bar: 100 μm); Similar number of the CFUs developed from the EDA-overexpressing cells and its controls; the CFUs were stained with 0.1% crystal violet (**c1**, **c2**). There were accelerated migration of EDA-overexpressing cells from the 0 to the 24th hours (**d1**, **e1**), compared with the controls (**d2**, **e2**); and more cells overexpressing recombinant EDA (**f1**) than the controls (**f2**) crossed over the transwell inserts membrane (with original magnification ×100, scale bar: 100 μm). As the EDA overexpression increased cellular motility (**g1**, **h1**), it was stained with more intensed F-actin than the controls (**g2**, **h2**) (with original magnification ×100 and 200, scale bar: 100 and 50 μm). The F-actin filaments concentrated in the increased ruffles and lamellipodia as the EDA overexpressing (**i1**); the controls exhibited less F-actin filaments, ruffles, and lamellipodia (**i2**) (with original magnification ×400, scale bar: 20 μm)

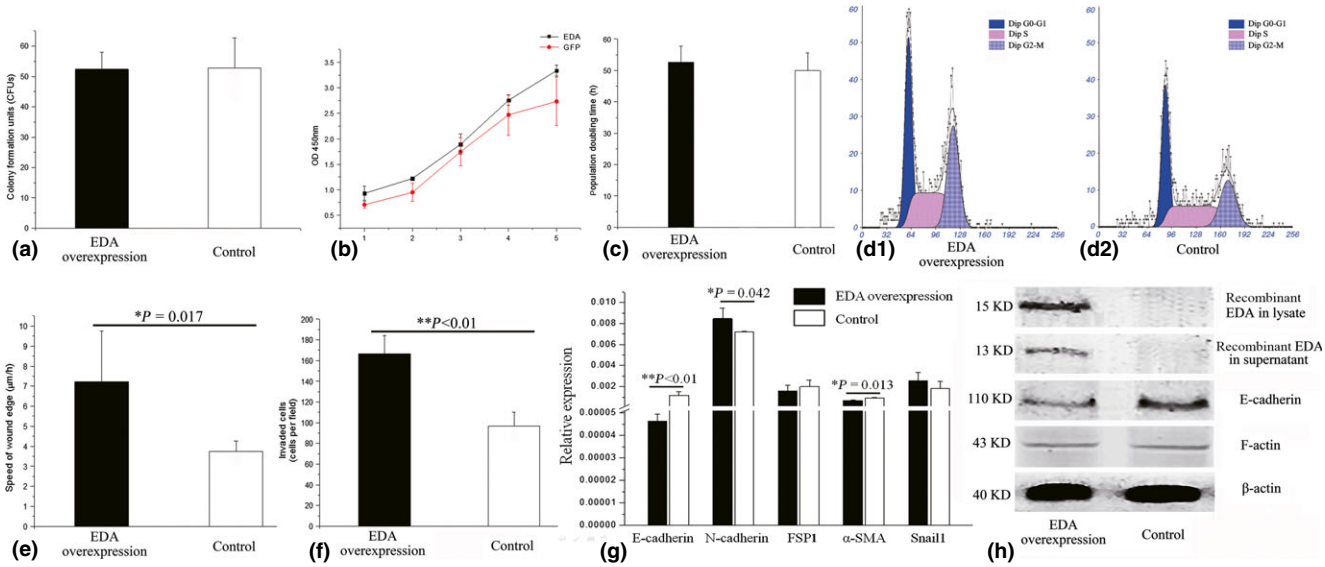

Figure 2 The overexpression of recombinant EDA exhibited no significant effects on the growth of SACC cells, as illustrated in CFUs counting (**a**), cellular proliferation curves (**b**), PDT (**c**) as well as cell cycle distribution (**d1**, **d2**). But the effects of overexpressed EDA significantly increased the cellular motility ($P < 0.05$) (**e**) and aggressiveness ($P < 0.01$) (**f**). Correspondingly, the mRNA levels of genes regulating EMT were different with that in the controls (**g**). The recombinant EDA protein and correspondingly changed E-cadherin were demonstrated with Western blot, but the F-actin remained similar to controls (**h**)

Table 3 The cell cycle distribution of the EDA-overexpressing cells and its control

Groups	*G0/G1 phase*	*S phase*	*G2-M phase*	*S+G2 phase*
EDA overexpression	34.30 ± 2.06	33.63 ± 1.20	32.08 ± 2.09	65.70 ± 2.06
Control	36.29 ± 2.64	35.58 ± 0.99	28.13 ± 2.71	63.71 ± 2.64
P	0.361718082	0.10694516	0.116355077	0.361718082

Table 4 The normalized expression of genes in EDA-overexpressing cells and its control

Genes	*EDA overexpression*	*Control*	P
E-cadherin	0.0000462261 ± 3.19077E-6	0.00117 ± 3.40155E-4	**<0.01
N-cadherin	0.00846 ± 9.77771E-4	0.00719 ± 1.05117E-4	*0.041
FSP1	0.00158 ± 5.77443E-4	0.002 ± 6.13311E-4	0.357
α-SMA	6.71134E-4 ± 8.07876E-5	8.89191E-4 ± 9.64479E-5	*0.013
Snail1	0.00255 ± 7.89961E-4	0.0018 ± 6.73081E-4	0.198

*$P < 0.05$.
**$P < 0.01$.

initiation of EMT induced by recombinant EDA; as a result, remodelled cytoskeleton increased the motility of SACC cells.

Expression profiles of EDA+FN in SACC tissue

Clinical characteristics of patients with SACC are shown in Table 5. EDA+FN was mainly expressed in the cytoplasm of cancer cells, and 53.1% (43/81) of SACC specimens displayed high expression and 46.9% (38/81) displayed low expression (Figure 3). The level of EDA+FN expression was significantly correlated with metastasis ($P = 0.012$), nerve invasion symptom ($P = 0.013$), and recurrence ($P = 0.041$), suggesting that high EDA+FN expression was related to higher incidence of metastasis (50%), nerve invasion (73.7%) as well as recurrence (52.6%) than low EDA+FN expression (23.3%, 46.5%, 30.2%). However, there were no significant correlations between EDA+FN expression and other clinicopathological factors, such as age ($P = 0.320$), gender ($P = 0.181$), tumor size ($P = 0.794$), and histological subtype ($P = 0.177$) (Table 5). Consistently, the H-scores in tissues of patients with metastasis, nerve invasion, and recurrence were also significantly higher than those without metastasis, nerve invasion, and recurrence (Figure 4a–c). However, patients with high expression of EDA+FN failed to display shorter overall survival rates and disease-free survival rates than those with low expression of EDA+FN ($P = 0.632$ &. $P = 0.374$) (Figure 4d1–d2).

Table 5 Correlation between EDA+FN expression and clinicopathological parameters in patients with SACC

Parameters	*Low EDA+FN expression*	*High EDA+FN expression*	χ^2 *value*	P-*value*
Age (years)				
≤50	24 (55.8%)	17 (44.7%)	0.99	0.32
>50	19 (44.2%)	21 (55.3%)		
Gender				
Male	10 (23.3%)	14 (36.8%)	1.786	0.181
Female	33 (76.7%)	24 (63.2%)		
Histological subtype				
Solid	8 (18.6%)	12 (31.6%)	1.826	0.177
Cribriform/tubular	35 (81.4%)	26 (68.4%)		
Metastasis				
Negative	33 (76.7%)	19 (50%)	6.278	*0.012
Positive	10 (23.3%)	19 (50%)		
Tumor size				
≤2 cm	18 (41.9%)	17 (44.7%)	0.068	0.794
>2cm	25 (58.1%)	21 (55.3%)		
Nerve invasion				
Yes	20 (46.5%)	28 (73.7%)	6.169	*0.013
No	23 (53.5%)	10 (26.3%)		
Recurrence				
Yes	13 (30.2%)	20 (52.6%)	4.192	*0.041
No	30 (69.8%)	18 (47.4%)		

*$P < 0.05$.
**$P < 0.01$.

The EDA exon was excluded from the FN gene by the CRISPR/Cas9 system

Genomic DNA was extracted from the SACC-83 cells co-transfected with two sgRNA-guided CRISPR/Cas9 plasmids, in which these 2 sgRNAs targeted the upstream and downstream sites of EDA exon, respectively. PCR amplification of genomic DNA was performed with the primers complemented to the sequences flanking the double strain breaks (DSBs) to access the efficiency of gene editing (Figure 4e1–e6). The PCR products amplified from the EDA-knockout genomic DNA revealed the length of 415 bp, and those from the EDA-positive genomic DNA generated a 675-bp fragment equal to that of control cells. The width and light intensity ratio of the two bands indicated that the majority of cells lost their EDA exon (Figure 4j). DNA sequencing confirmed that the PCR product (415 bp) was corresponding to the EDA-knockout FN gene sequence (Figure 4f1–f2).

Consistently, the SACC cells co-transfected with CRISPR/Cas9 plasmids expressed low level of EDA+FN, but the total amount of fibronectin was still approximate to control SACC-83 cells (Figure 4n). These results suggested that the two sgRNA-guided CRISPR/Cas9 plasmids could effectively eliminate EDA exon from SACC genome without side effects on the total expression of FN. In addition, our study also showed that the efficiency of EDA knockout could maintain at least 10 passages as described previously (Wang *et al*, 2013).

EDA exon knockout decreased the cell motility accompanied with downregulated EMT

Contrary to overexpressed recombinant EDA, the exclusion of EDA in SACC cells resulted in a significant decrease in cell motility compared with untreated SACC-83 cells (9.133 ± 1.58 μm h^{-1} *vs* 14.2 ± 1.36 μm h^{-1}, $P < 0.01$) (Figures 4k and 5e1–f2); decreased invasive ability resulted from the lack of EDA, compared with untreated SACC-83 cells (146.75 ± 40.49 per field *vs* 216.75 ± 39.17 per field, $P < 0.01$) (Figures 4l and 5g1–g2). Although the majority of both EDA-knockout and untreated cells displayed polygonal morphology, the former exhibited relatively weak F-actin staining (Figure 5c1–d2), less membrane ruffles, and lamellipodia than the latter (Figure 5h1–h2). As shown in Table 6, both the mRNA and protein levels of E-cadherin were significantly higher in EDA-knockout cells than untreated cells (Figure 4n), suggesting that the exclusion of EDA exon impaired the motility and aggressiveness of SACC cells via downregulated EMT.

Effects of EDA exclusion on the growth of SACC cells

The CFU counting was similar between EDA-knockout and untreated SACC-83 cells (149 ± 17.52/400 cells *vs* 144.1 ± 21.79/400 cells, $P = 0.699$) (Figures 4g and 5b1–b2); and little difference in the proportion of cells at the G0/G1, S, and G2/M phases between these two groups (Figure 5a1–a2 and Table 7). But the PDT was significantly prolonged in EDA-knockout cells compared with untreated cells (52.22 ± 1.34 h *vs* 46.33 ± 2.49 h, $P = 0.023$) (Figure 4h, i). It is possible that the effect of EDA on the cell proliferation is receptor dependent and that EDA overexpression exhibited little promotion because of limited receptors, but the shortage of EDA decreased the growth rate.

Discussion

Several lines of evidence have suggested that the EDA exon has a positive correlation with metastasis and poor prognosis in various cancers (Ou *et al*, 2014; Sun *et al*, 2014), but its role in SACC remains unclear. In this study, we confirmed that overexpression of recombinant EDA in SACC cells promoted migration and invasion (Figures 1d1–f2 and 2e, f and h). Meanwhile, downregulated E-cadherin, an molecule maintaining adhesion between epithelial cells (Zeisberg and Neilson, 2009), suggested the initiation of EMT in EDA-overexpressing SACC cells. Although the total amount of F-actin seemed similar (Figure 2h), the EDA overexpressing cells became thickly stained, ruffled, and formed lamellipodia as a result of redistribution of F-actin filament, which reflects the morphological changes during EMT (Caja *et al*, 2007) (Figure 1g1–i2). There were little effects of EDA on the growth PDT and CFU counting of SACC cells, although the proliferation index (PI = G2/M+S%) has been investigated (Figures 1c1–c2 and 2a–d2). These observations suggest that the main role of EDA in SACC cells is to facilitate motility and invasion; instead of proliferation, it is possibly involved in aggressiveness and metastasis of cancer.

In line with the above observations, the expression of EDA+FN in cases of SACC with metastasis was significantly higher than that in cases of SACC without metastasis (Figures 3a1–b2 and 4a), leading to the recurrence of

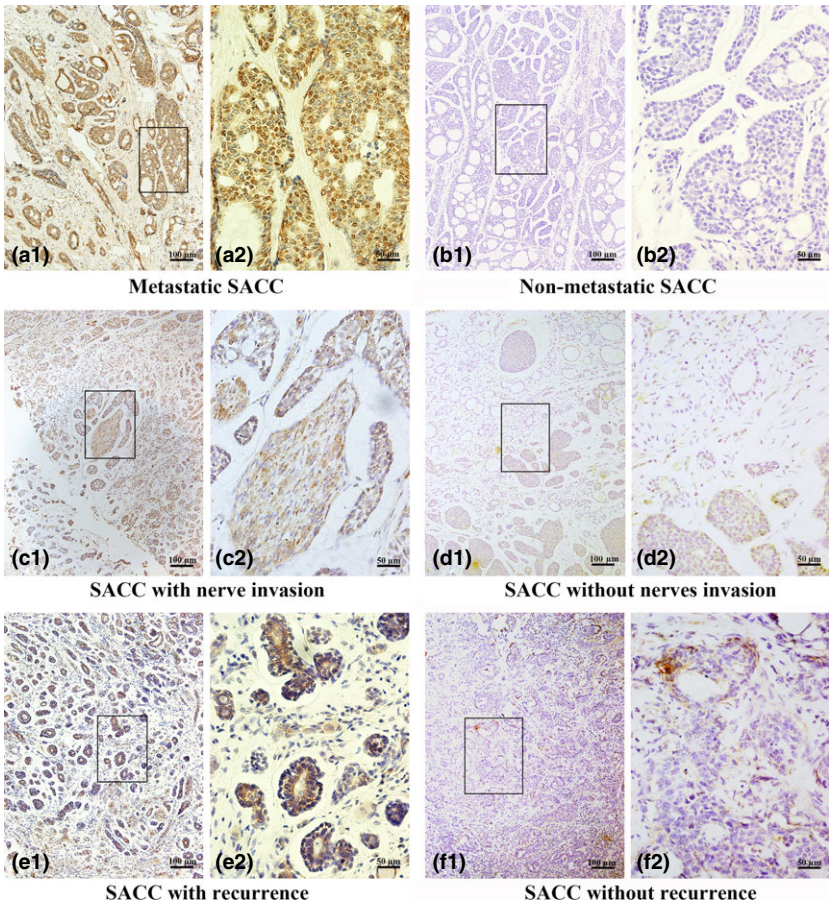

Figure 3 The EDA+FN appeared as brown particles mainly in cytoplasm of SACC, occasionally in cancer stroma. In the groups of SACC patients with metastasis (**a1**, **a2**), nerve invasion (**c1**, **c2**), and recurrence (**e1**, **e2**), more intense immunostaining of EDA+FN was investigated, as compared to their controls without the metastasis (**b1**, **b2**), nerve invasion (**d1**, **d2**) as well as recurrence (**f1**, **f2**), respectively. (with original magnification ×100 and 200, scale bar: 100 and 50 μm)

cancer (Figures 3e1–f2 and 4c) or to the symptoms of nerves invasion such as pain, numb, and tickle (Figures 3c1–d2 and 4b) in some cases. However, the EDA+FN staining did not appear to be associated with tumor sizes, gender, age, and histological subtype (Table 5). While EDA showed progrowth effects on nasopharyngeal carcinomas, colorectal cancer, and lymphatic endothelial cells (Ou *et al*, 2010, 2012; Sun *et al*, 2014), little contribution of EDA to SACC growth may be due to the slow growth rate of SACC cells themselves (Moskaluk, 2013). As the EDA exon facilitates SACC migration both *in vitro* and *in vivo*, it is likely to be a valuable target for inhibition of SACC aggressiveness and metastasis.

Alternative splicing provides potentials to generate diverse variants and ubiquitously participates in the progress of cancer (David and Manley, 2010). Therefore, how to control the alternative splicing of EDA becomes particularly valuable for the treatment of SACC as well as other cancers (Ou *et al*, 2010, 2012). The siRNA molecules have already been utilized to knock down some abnormally spliced variants, for example knockdown of KLF6-SV1 (Narla *et al*, 2005) or MNK2, making cancer cells more sensitive to anti-cancer drugs (Adesso *et al*, 2013), but siRNA is likely to break down the whole mRNA of EDA+FN instead of a specific target sequence (Gomes-da-Silva *et al*, 2014), so that the siRNA treatment could result in side effects caused by the degradation of entire FN sequences, because the parts outside of EDA domain is vital to normal tissues (White *et al*, 2008).

Recently, the type II bacterial clustered, regularly interspaced, palindromic repeats (CRISPR)-associated (Cas) system has provided a new method to edit genomic DNA. This system has been engineered into a single plasmid consisting of Cas9 nuclease, tracrRNA, and a single-guide RNA (sgRNA) sequence, that is the CRISPR/Cas9 system (Cho *et al*, 2013; Hsu *et al*, 2013; Pyzocha *et al*, 2014). The sgRNA containing 20-nucleotide (nt) complements the target region of DNA with a 5′-NGG-3′ protospacer-adjacent motif (PAM), and the linked tracrRNA recruited nuclease Cas9 to generate the double-strand DNA breaks (DSBs) at target sites, which would be repaired by either non-homologous end-joining (NHEJ) or homology-directed repair (HDR) subsequently (Wang *et al*, 2013) (Figure 4e1–e6). The CRISPR/Cas9 system has been applied to correct disease-causing mutations for cataract and cystic fibrosis (Schwank *et al*, 2013) in mouse zygotes and human cell lines as well as to correct tyrosinemia in adult mammalian liver (Yin *et al*, 2014). Therefore, the CRISPR/Cas system is likely valuable to be used in treating the pro-oncogenic splicing exon, such as EDA.

According to the study reported by Wang *et al* (2013), we designed two sgRNA sequences to target the upstream and downstream sequences of human EDA exon and, respectively, integrated them into pX330 CRISPR vectors containing the recombinant Cas9. The two vectors were cotransfected into SACC-83 cells, and primers flanking the target loci of sgRNA were used to illustrate the knockout efficiency (Figure 4e1–e6). According to previous

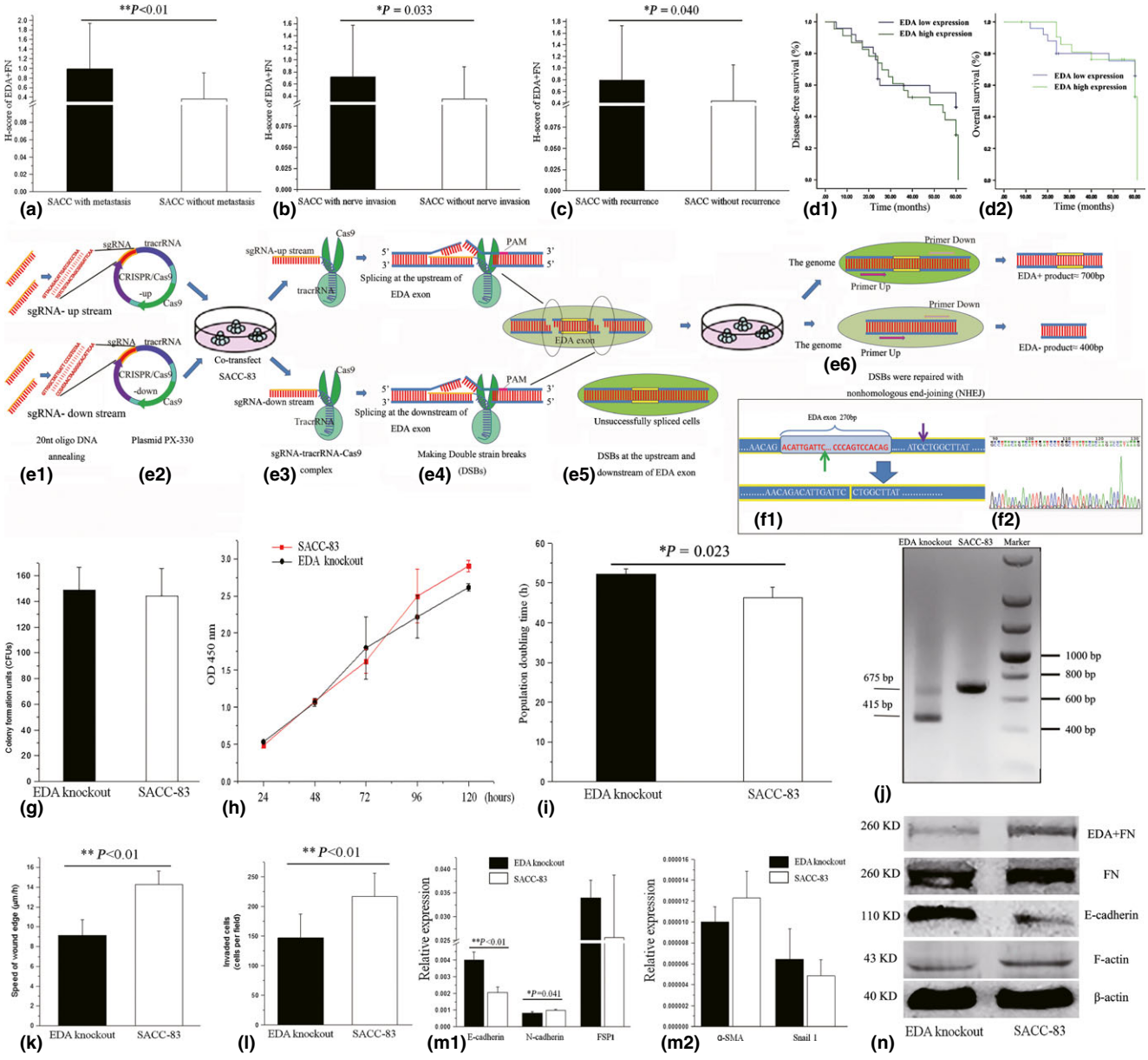

Figure 4 The H-score of EDA+FN staining in the SACC tissues with metastasis, nerve invasion, and recurrence is significantly higher than that in the tissue of the patients without such symptoms, respectively ($P < 0.05$) (**a**–**c**), despite the expression level of EDA+FN did not exhibited significantly associations with the rate of disease-free survival and overall survival (**d1**, **d2**). To eliminate the EDA exon from the FN gene, the CRISPR/Cas9 system was designed and used to generate DSBs flanking EDA exon, as illustrated in (**e1**–**e6**); the efficiency of EDA knockout was demonstrated by PCR (**j**) as well as DNA sequencing (**f1**–**f2**). As a result of EDA knockout, despite the still approximate CFUs counting (**g**), the proliferation decreased and PDT prolonged significantly in contrast with the untreated SACC-83 ($P < 0.05$) (**h**, **i**). In addition, both the cellular motility and aggressiveness significantly decreased in the EDA-knockout group, compared with untreated SACC-83 ($P < 0.01$) (**k**, **l**); it was also accompanied with changed mRNA levels of genes regulating EMT (**m1**, **m2**). The decreased EDA+FN and E-cadherin was demonstrated by Western blot; however, the total amount of FN and F-actin seemed approximate between EDA-knockout and untreated SACC-83 cells (**n**)

Table 6 The normalized expression of genes in EDA-knockout cells and SACC-83

Genes	*EDA knockout*	*SACC-83*	P
E-cadherin	0.00205 ± 3.24607E-4	0.004 ± 4.84503E-4	**<0.01
N-cadherin	9.72913E-4 ± 7.69101E-5	8.19957E-4 ± 8.92934E-5	*0.040
FSP1	0.02566 ± 0.01306	0.03396 ± 0.00374	0.267
α-SMA	1.22698E-5 ± 2.58212E-6	1.00117E-5 ± 1.44193E-6	0.178
Snail1	4.8395E-6 ± 1.5464E-6	6.45447E-6 ± 2.90763E-6	0.365

*$P < 0.05$.
**$P < 0.01$.

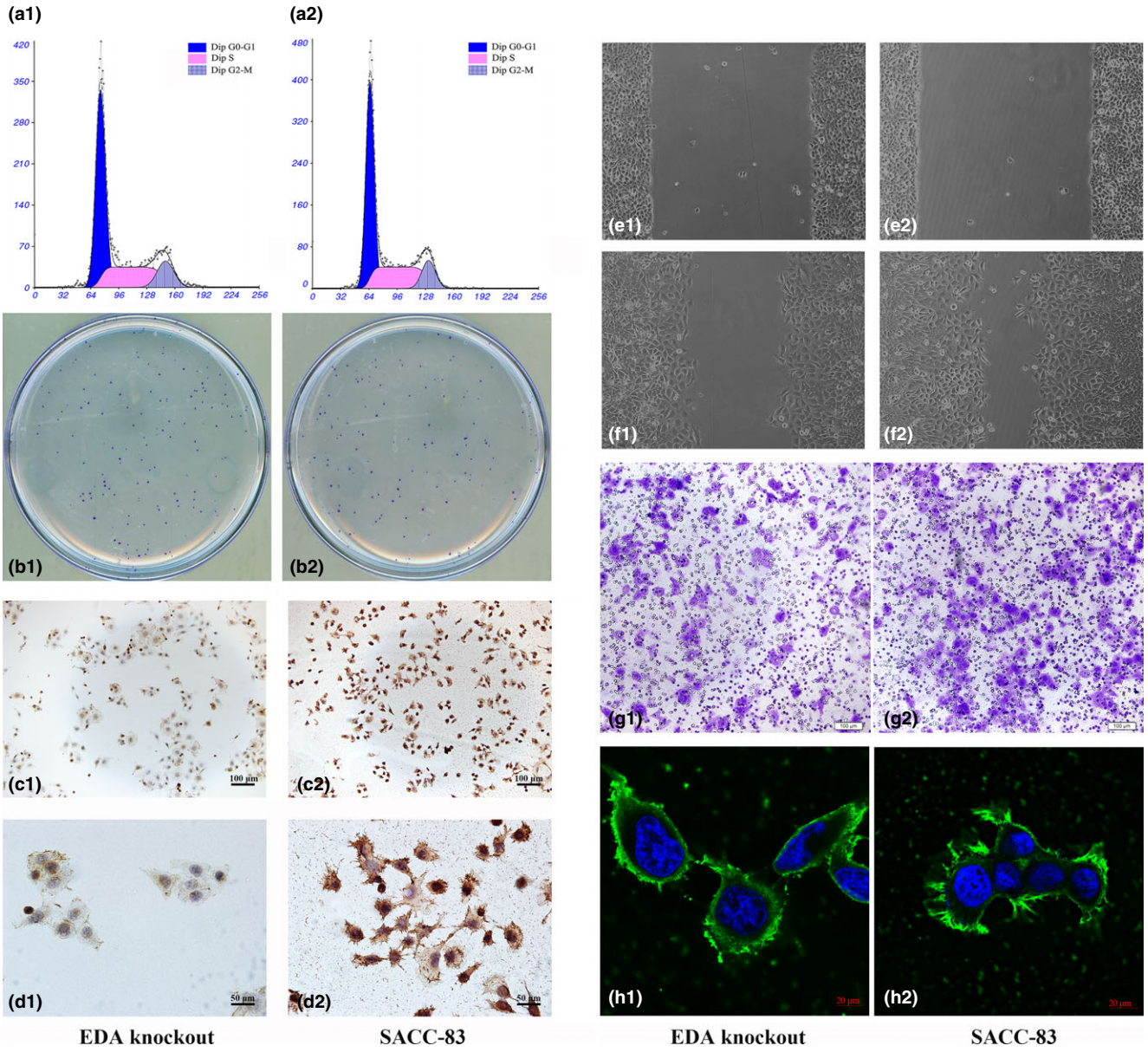

Figure 5 Although both the cell cycle distribution (**a1**, **a2**) and CFUs (**b1**, **b2**) counting seemed not influenced by the EDA exclusion, it indeed resulted in weaker staining of F-actin (**c1**, **d1**), compared with untreated SACC-83 (**c2**, **d2**) (with original magnification ×100 and 200, scale bar: 100 and 50 μm). Therefore, the cellular migration of EDA-knockout cells (**e1**–**f1**) is slower than that of untreated SACC-83 from the 0 to the 24th hours (**e2**, **f2**); as well as less EDA-knockout cells (**g1**) crossed over the transwell inserts membrane than untreated SACC-83 (**g2**) (with original magnification ×100, scale bar: 100 μm). Despite both groups of cells tend to displayed polygonal morphology, the EDA-knockout cells (**h1**) still exhibited less membrane ruffles and lamellipodia than untreated SACC-83 (**h2**), in which the F-actin concentrated in the extrusions (with original magnification ×400, scale bar: 20 μm)

Table 7 The cell cycle distribution of the EDA-knockout cells and the control SACC-83 cells

Groups (n = *3*)	*G0/G1 phase*	*S phase*	*G2-M phase*	*S+G2 phase*
EDA knockout	58.614 ± 7.109	31.101 ± 3.743	12.264 ± 2.015	43.365 ± 1.799
SACC-83	63.165 ± 4.796	25.930 ± 2.341	11.372 ± 1.775	37.302 ± 4.083
P	0.410042882	0.112373563	0.596173078	0.078234752

*$P < 0.05$.
**$P < 0.01$.

study (Cho *et al*, 2013), optical density between 675 and 400 bp bands reflects the majority of cells lost EDA exon, and DNA sequencing indicated the DSBs of EDA elimination was repaired by NHEJ (Figure 4f1–f2 and j). Decreased EDA+FN and approximate total FN were confirmed in Western blot (Figure 4j, n), suggesting the

CRISPR/Cas9 system is an effective tool of editing genome directly without significantly side effects on the total amount of FN.

Although the total amount of FN seemed approximate between EDA-knockout cells and untreated SACC-83 cells, the former displayed longer PDT, which is inconsistent with the finding that EDA overexpression may not affect cell growth (Figure 4h–i). Possibly, the effect of EDA on SACC growth is receptor dependent, such as integrin $\alpha 9\beta 1$ (Liao *et al*, 2002). The lack of EDA may therefore result in downregulated proliferation, while excess EDA did nothing because of limited receptors. In addition, EDA knockout leads to decreased motility and invasion of SACC cells (Figures 4k–l and 5e1–g2), accompanied with increased E-cadherin, decreased F-actin staining cells, and lamellipodia with less assembled F-actin filament (Caja *et al*, 2007; Zeisberg and Neilson, 2009) (Figures 4m1–n and 5c1–d2, h1–h2), suggesting downregulated EMT. Therefore, the CRISPR/Cas9 system can effectively control the growth and migration of SACC cells by direct knockout of EDA exon from the FN gene.

In summary, the alternative splicing exon EDA domain can promote the motility of SACC cells, and EDA+FN is positively associated with the metastasis, nerve invasion, and recurrence of SACC. The CRISPR/Cas9 system could directly eliminate such a pro-oncogenic exon from genome. With further improved knockout specificity and drug vehicle (Ran *et al*, 2013), the CRISPR/Cas system would be a promising therapeutic approach to the control of pro-oncogenic splicing-induced tumors (Yin *et al*, 2014).

Acknowledgement

This work was supported by National Nature Science Foundation of China (No. 81072214) and (No. 81171006).

Author contributions

Hai-cheng Wang, contributed to: the study concepts and design, the clinical studies, the literature and experimental researches, data acquisition and analysis, manuscript preparation and editing. Yue-Yang, contributed to: the clinical studies, the literature and experimental researches, data acquisition and analysis. Shu-yu Xu, contributed to: the clinical studies, the literature and experimental researches. Jing Peng, contributed to: the clinical studies, the literature and experimental researches. Jiu-hui Jiang, contributed to: the study concepts and design, guarantee of the integrity of study, manuscript editing and review. Cui-ying Li, contributed to: the study concepts and design, guarantee of the integrity of study, clinical study, data analysis, manuscript preparation, editing and review.

Conflict of interest

None declared.

References

Adesso L, Calabretta S, Barbagallo F *et al* (2013). Gemcitabine triggers a pro-survival response in pancreatic cancer cells through activation of the MNK2/eIF4E pathway. *Oncogene* **32**: 2848–2857.

Bauman JA, Li SD, Yang A, Huang L, Kole R (2010). Anti-tumor activity of splice-switching oligonucleotides. *Nucleic Acids Res* **38**: 8348–8356.

Bonomi S, Gallo S, Catillo M, Pignataro D, Biamonti G, Ghigna C (2013). Oncogenic alternative splicing switches: role in cancer progression and prospects for therapy. *Int J Cell Biol* **2013**: 962038.

Budwit-Novotny DA, McCarty KS, Cox EB *et al* (1986). Immunohistochemical analyses of estrogen receptor in endometrial adenocarcinoma using a monoclonal antibody. *Cancer Res* **46**: 5419–5425.

Caja L, Ortiz C, Bertran E *et al* (2007). Differential intracellular signalling induced by TGF-beta in rat adult hepatocytes and hepatoma cells: implications in liver carcinogenesis. *Cell Signal* **19**: 683–694.

Cho SW, Kim S, Kim JM, Kim JS (2013). Targeted genome engineering in human cells with the Cas9 RNA-guided endonuclease. *Nat Biotechnol* **31**: 230–232.

Cong L, Ran FA, Cox D *et al* (2013). Multiplex genome engineering using CRISPR/Cas systems. *Science* **339**: 819–823.

Dai W, Yao Y, Zhou Q, Sun CF (2014). Ubiquitin-specific peptidase 22, a histone deubiquitinating enzyme, is a novel poor prognostic factor for salivary adenoid cystic carcinoma. *PLoS ONE* **9**: e87148.

David CJ, Manley JL (2010). Alternative pre-mRNA splicing regulation in cancer: pathways and programs unhinged. *Genes Dev* **24**: 2343–2364.

Davuluri RV, Suzuki Y, Sugano S, Plass C, Huang TH (2008). The functional consequences of alternative promoter use in mammalian genomes. *Trends Genet* **24**: 167–177.

Dong L, Wang YX, Li SL *et al* (2011). TGF-beta1 promotes migration and invasion of salivary adenoid cystic carcinoma. *J Dent Res* **90**: 804–809.

Dong L, Ge XY, Wang YX *et al* (2013). Transforming growth factor-beta and epithelial-mesenchymal transition are associated with pulmonary metastasis in adenoid cystic carcinoma. *Oral Oncol* **49**: 1051–1058.

El-Nagdy S, Salama NM, Mourad MI (2013). Immunohistochemical clue for the histological overlap of salivary adenoid cystic carcinoma and polymorphous low-grade adenocarcinoma. *Interv Med Appl Sci* **5**: 131–139.

Epivatianos A, Iordanides S, Zaraboukas T, Antoniades D (2005). Adenoid cystic carcinoma and polymorphous low-grade adenocarcinoma of minor salivary glands: a comparative immunohistochemical study using the epithelial membrane and carcinoembryonic antibodies. *Oral Dis* **11**: 175–180.

Gomes-da-Silva LC, Simoes S, Moreira JN (2014). Challenging the future of siRNA therapeutics against cancer: the crucial role of nanotechnology. *Cell Mol Life Sci* **71**: 1417–1438.

Guillot C, Lecuit T (2013). Mechanics of epithelial tissue homeostasis and morphogenesis. *Science* **340**: 1185–1189.

Hsu PD, Scott DA, Weinstein JA *et al* (2013). DNA targeting specificity of RNA-guided Cas9 nucleases. *Nat Biotechnol* **31**: 827–832.

Jinek M, Chylinski K, Fonfara I, Hauer M, Doudna JA, Charpentier E (2012). A programmable dual-RNA-guided DNA endonuclease in adaptive bacterial immunity. *Science* **337**: 816–821.

Li SL (1990). Establishment of a human cancer cell line from adenoid cystic carcinoma of the minor salivary gland. *Zhonghua Kou Qiang Yi Xue Za Zhi* **25**: 29–31, 62.

Liao YF, Gotwals PJ, Koteliansky VE, Sheppard D, Van De Water L (2002). The EIIIA segment of fibronectin is a ligand for integrins alpha 9beta 1 and alpha 4beta 1 providing a novel mechanism for regulating cell adhesion by alternative splicing. *J Biol Chem* **277**: 14467–14474.

Manabe R, Ohe N, Maeda T, Fukuda T, Sekiguchi K (1997). Modulation of cell-adhesive activity of fibronectin by the alternatively spliced EDA segment. *J Cell Biol* **139**: 295–307.

McFadden JP, Baker BS, Powles AV, Fry L (2010). Psoriasis and extra domain A fibronectin loops. *Br J Dermatol* **163**: 5–11.

Moskaluk CA (2013). Adenoid cystic carcinoma: clinical and molecular features. *Head Neck Pathol* **7**: 17–22.

Narla G, DiFeo A, Yao S *et al* (2005). Targeted inhibition of the KLF6 splice variant, KLF6 SV1, suppresses prostate cancer cell growth and spread. *Cancer Res* **65**: 5761–5768.

Nowak DG, Woolard J, Amin EM *et al* (2008). Expression of pro- and anti-angiogenic isoforms of VEGF is differentially regulated by splicing and growth factors. *J Cell Sci* **121**: 3487–3495.

Ou JJ, Wu F, Liang HJ (2010). Colorectal tumor derived fibronectin alternatively spliced EDA domain exserts lymphangiogenic effect on human lymphatic endothelial cells. *Cancer Biol Ther* **9**: 186–191.

Ou J, Li J, Pan F *et al* (2011). Endostatin suppresses colorectal tumor-induced lymphangiogenesis by inhibiting expression of fibronectin extra domain A and integrin alpha9. *J Cell Biochem* **112**: 2106–2114.

Ou J, Pan F, Geng P *et al* (2012). Silencing fibronectin extra domain A enhances radiosensitivity in nasopharyngeal carcinomas involving an FAK/Akt/JNK pathway. *Int J Radiat Oncol Biol Phys* **82**: e685–e691.

Ou J, Peng Y, Deng J *et al* (2014). Endothelial cell-derived fibronectin extra domain A promotes colorectal cancer metastasis via inducing epithelial-mesenchymal transition. *Carcinogenesis* **35**: 1661–1670.

Pal S, Gupta R, Davuluri RV (2012). Alternative transcription and alternative splicing in cancer. *Pharmacol Ther* **136**: 283–294.

Pyzocha NK, Ran FA, Hsu PD, Zhang F (2014). RNA-guided genome editing of mammalian cells. *Methods Mol Biol* **1114**: 269–277.

Rajan P, Elliott DJ, Robson CN, Leung HY (2009). Alternative splicing and biological heterogeneity in prostate cancer. *Nat Rev Urol* **6**: 454–460.

Ran FA, Hsu PD, Lin CY *et al* (2013). Double nicking by RNA-guided CRISPR Cas9 for enhanced genome editing specificity. *Cell* **154**: 1380–1389.

Schwank G, Koo BK, Sasselli V *et al* (2013). Functional repair of CFTR by CRISPR/Cas9 in intestinal stem cell organoids of cystic fibrosis patients. *Cell Stem Cell* **13**: 653–658.

Shinde AV, Bystroff C, Wang C *et al* (2008). Identification of the peptide sequences within the EIIIA (EDA) segment of fibronectin that mediate integrin alpha9beta1-dependent cellular activities. *J Biol Chem* **283**: 2858–2870.

van der Straaten HM, Canninga-van Dijk MR, Verdonck LF *et al* (2004). Extra-domain-A fibronectin: a new marker of fibrosis in cutaneous graft-versus-host disease. *J Invest Dermatol* **123**: 1057–1062.

Sun W, Ye Z, Mi Z, Shi T, Han C, Guo S (2008). A comparative study on proteomics between LNCap and DU145 cells by quantitative detection and SELDI analysis. *J Huazhong Univ Sci Technolog Med Sci* **28**: 174–178.

Sun X, Fa P, Cui Z *et al* (2014). The EDA-containing cellular fibronectin induces epithelial-mesenchymal transition in lung cancer cells through integrin alpha9beta1-mediated activation of PI3-K/AKT and Erk1/2. *Carcinogenesis* **35**: 184–191.

Vargas PA, Speight PM, Bingle CD, Barrett AW, Bingle L (2008). Expression of PLUNC family members in benign and malignant salivary gland tumours. *Oral Dis* **14**: 613–619.

Wang HC, Li TJ (2013). The growth and osteoclastogenic effects of fibroblasts isolated from keratocystic odontogenic tumor. *Oral Dis* **19**: 162–168.

Wang H, Yang H, Shivalila CS *et al* (2013). One-step generation of mice carrying mutations in multiple genes by CRISPR/Cas-mediated genome engineering. *Cell* **153**: 910–918.

Wang H.C., Jiang W.P., Sima Z.H., Li T.J. (2014). Fibroblasts isolated from a keratocystic odontogenic tumor promote osteoclastogenesis in vitro via interaction with epithelial cells. *Oral Dis* **21**: 170–177.

White ES, Baralle FE, Muro AF (2008). New insights into form and function of fibronectin splice variants. *J Pathol* **216**: 1–14.

Yin H, Xue W, Chen S *et al* (2014). Genome editing with Cas9 in adult mice corrects a disease mutation and phenotype. *Nat Biotechnol* **32**: 551–553.

Zeisberg M, Neilson EG (2009). Biomarkers for epithelial-mesenchymal transitions. *J Clin Invest* **119**: 1429–1437.

Zhang JP, Li CY (2007). The effect of transforming growth factor-beta1 on EDA region of fibronectin in oral squamous cell carcinoma and adenoid cystic carcinoma cells. *Zhonghua Kou Qiang Yi Xue Za Zhi* **42**: 47–51.